

Table 3. Clinical characteristics of 13 patients with HCC after SVR to IFN therapy at the time of detection of HCC

	Sex	Age	Interval* (months)	Laboratory data				Elevated tumor marker
				T-Bil (mg/dl)	Alb (g/dl)	PT (%)	ALT (IU/l)	
1	M	66	13	0.5	4	108	18	AFP
2	M	71	36	0.3	4.2	NA	18	-
3	M	59	33	0.7	3.9	127	14	PIVKA-II
4	M	67	85	0.9	4.3	88	23	-
5	M	67	81	0.7	4.1	73	59	PIVKA-II
6	M	55	83	0.9	4	86	19	PIVKA-II
7	M	59	17	1.9	3.6	NA	27	AFP
8	M	67	71	0.6	5	96	57	-
9	M	67	71	1.1	4.7	80	25	AFP,PIVKA-II
10	M	54	115	1.2	5	93	46	NA
11	M	69	45	1.2	3.7	98	88	AFP,PIVKA-II
12	M	71	104	0.8	4.5	93	62	AFP,PIVKA-II
13	M	69	144	0.5	4	99	31	PIVKA-II

HCC					
	No.	Size (mm)	Differentiation	Therapy	Recurrence
1	1	15	Moderate	operation	+
2	2	15	Well	PEI	+
3	3	27	Moderate	operation	+
4	1	32	NA	-	NA
5	1	16	Moderate	operation	-
6	1	20	NA	TAE+RFA	-
7	2	30	Poor	operation	+
8	1	30	Moderate	operation	-
9	1	13	NA	RFA	-
10	1	21	NA	RFA	-
11	1	110	Poor	operation	+
12	2	57	NA	TAE	-
13	1	30	Moderate	operation	-

*Interval from the end of IFN therapy to the detection of HCC.

NA, not available; PEI, percutaneous ethanol injection; TAE, transcatheter arterial embolization; RFA, radiofrequency ablation; T-Bil, total bilirubin; Alb, albumin; PT, prothrombin time; ALT, alanine aminotransferase; HCC, hepatocellular carcinoma; AFP, α -fetoprotein; PIVKA-II, protein-induced vitamin K absence or antagonist II.

ethanol injection therapy, radiofrequency ablation, or a combination of these treatments. One patient refused further therapy. HCC recurred in other areas of the liver in five patients. Two patients died from progression of HCC (cases 3 and 11).

Discussion

Since 1992, IFN therapy has been covered by National Health Insurance in Japan. To date, about 400 000 patients with CH-C have received IFN, including about 70 000 concurrently given ribavirin, launched in 2001. With a combination of pegylated IFN and ribavirin, more than 50% of patients with CH-C have SVR (24, 25). It has thus become very important to

establish follow-up protocols for patients with CH-C who have SVR to IFN therapy.

Although complete eradication of HCV by IFN therapy significantly reduces the incidence of HCC, previous studies have shown that HCC develops in 2.5–4.2% of patients with SVR (18, 19, 22). In our study, the incidence of HCC among 373 SVR patients was 3.5% during a median follow-up period of 66 months (range, 12–197 months). Some groups previously reported that HCCs in patients with SVR (if any) are usually detected within 5 years after the end of IFN therapy and speculated that HCC was already present but too small to be detected before the start of therapy (19). However, the mean interval from the completion of IFN therapy to the detection of HCC in

our SVR patients was about 5.8 years. Moreover, in eight of the 13 SVR HCC patients, HCC was detected more than 5 (up to 12) years after the end of IFN therapy. In addition, the interval to the detection of HCC did not significantly differ between SVR HCC patients and non-SVR HCC patients. The discrepancy between our findings and the results of previous studies might be due to the longer observation period in our study.

Among patients with SVR, advanced age, male sex, and advanced histologic stage of disease have been linked to an increased risk for the development of HCC (19). Consistent with these previous findings, we found that male sex, advanced age, and advanced hepatic fibrosis were important risk factors, although in nearly half of the patients liver biopsy was not performed. Of the 13 SVR HCC patients, however, HCC developed in three with mild fibrosis (F1) after IFN therapy (cases 1–3 in Table 3). Moreover, HCC recurred in all three of these patients after operation or ablation therapy, including one who died of HCC progression. These patients neither abused alcohol nor had a history of blood transfusion, obesity, or diabetes mellitus. Their serum ALT levels were within the normal range. We have not been able to identify other characteristics of SVR HCC with mild fibrosis. These findings indicate that patients with SVR should be carefully observed for more than 10 years after the completion of IFN therapy, even if only early fibrosis is present.

Because liver function is well maintained after the elimination of HCV, most patients with SVR can receive curative treatment such as hepatic resection, provided that HCC is detected at an early stage. At the time of diagnosis of HCC, all of our patients were negative for HCV RNA and most had a good hepatic reserve. However, some patients had poor prognoses, despite curative therapy. Perhaps, some SVR patients did not return for follow-up because they considered their disease cured and were therefore not screened for HCC, resulting in delayed detection.

Chronic infection with HCV or hepatitis B virus (HBV) is the major cause of HCC in Japan; approximately 80% of HCCs are caused by HCV-associated chronic liver diseases, whereas the remaining 20% are positive for hepatitis B surface antigen (26). The mechanism of hepatocarcinogenesis in patients with SVR remains unclear. Occult infection with HBV (20) or HCV (27–29) may be one carcinogenic factor. Although occult HCV infection was not studied in our patients, HBV DNA integration was detected in one (case 5 in Table 3) of the three patients in whom viral integration was assessed (data not shown). Alco-

hol abuse, diabetes mellitus, and non-alcoholic steatohepatitis are also considered risk factors for HCC (30–33). Although environmental carcinogens such as aflatoxin B1 increase the risk of liver cancer in some countries, there is no evidence linking aflatoxin B1 or other chemical agents to HCC in Japan (34). Further studies are required to quantify the risk of HCC developing in patients after eradication of HCV.

In conclusion, patients with CH-C who are elderly, male, or have an advanced histological stage of disease remain at a high risk for HCC after having SVR to IFN therapy. We recommend that SVR patients, including those with early fibrosis, are carefully observed for more than 10 years after the completion of IFN therapy. Prospective studies are required to establish reliable follow-up protocols for patients with CH-C who have SVR to IFN therapy.

Acknowledgement

The authors thank Dr. Takashi Tanaka for providing statistical suggestions.

References

1. Bruix J, Barrera JM, Calvet X, *et al.* Prevalence of antibodies to hepatitis C virus in Spanish patients with hepatocellular carcinoma and hepatic cirrhosis. *Lancet* 1989; **II**: 1004–6.
2. Colombo M, Kuo G, Choo QL, *et al.* Prevalence of antibodies to hepatitis C virus in Italian patients with hepatocellular carcinoma. *Lancet* 1989; **II**: 1006–8.
3. Hoofnagle JH, Mullen KD, Jones DB, *et al.* Treatment of chronic hepatitis non-A, non-B hepatitis with recombinant human alpha interferon. *N Engl J Med* 1986; **315**: 1575–8.
4. Nishiguchi S, Kuroki T, Nakatani S, *et al.* Randomised trial of effects of interferon-alpha on incidence of hepatocellular carcinoma in chronic active hepatitis C with cirrhosis. *Lancet* 1996; **346**: 1051–5.
5. International Interferon-Hepatocellular Carcinoma Study Group. Effect of interferon-alpha on progression of cirrhosis to hepatocellular carcinoma: a retrospective cohort study. *Lancet* 1998; **35**: 1535–9.
6. Kasahara A, Hayashi N, Mochizuki K, *et al.* Risk factors for hepatocellular carcinoma and its incidence after interferon treatment in patients with chronic hepatitis C. Osaka Liver Disease Study Group. *Hepatology* 1998; **27**: 1394–402.
7. Yoshida H, Shiratori Y, Moriyama M, *et al.* Interferon therapy reduces the risk for hepatocellular carcinoma: national surveillance program of cirrhotic and noncirrhotic patients with chronic hepatitis C in Japan. *Ann Intern Med* 1999; **13**: 174–81.
8. Imai Y, Kawata S, Tamura S, *et al.* Relation of interferon therapy and hepatocellular carcinoma in patients with chronic hepatitis C. *Ann Intern Med* 1998; **129**: 94–99.

9. Yoshida H, Tateishi R, Arakawa Y, *et al.* Benefit of interferon therapy in hepatocellular carcinoma prevention for individual patients with chronic hepatitis C. *Gut* 2004; 53: 425–30.
10. Coverdale SA, Khan MH, Byth K, *et al.* Effects of interferon treatment response on liver complications of chronic hepatitis C: 9-year follow-up study. *Am J Gastroenterol* 2004; 99: 636–44.
11. Okanoue T, Itoh Y, Minami M, *et al.* Interferon therapy lowers the rate of progression to hepatocellular carcinoma on chronic hepatitis C but not significantly in an advanced stage: a retrospective study in 1148 patients. *J Hepatol* 1999; 30: 653–9.
12. Ikeda K, Saitoh S, Arase Y, *et al.* Effect of interferon therapy on hepatocellular carcinogenesis in patients with chronic hepatitis type C: long-term observation study of 1,643 patients using statistical bias correction with proportion hazard analysis. *Hepatology* 1999; 29: 1124–30.
13. Tanaka H, Tsukuma H, Kasahara A, *et al.* Effect of interferon therapy on the incidence of hepatocellular carcinoma and mortality of patients with chronic hepatitis C: a retrospective cohort study of 738 patients. *Int J Cancer* 2000; 87: 741–9.
14. Tamori A, Kuroki T, Nishiguchi S, *et al.* Case of hepatocellular carcinoma in the caudate lobe detected after interferon caused disappearance of hepatitis C virus. *Hepatogastroenterology* 1996; 43: 1079–83.
15. Kim SR, Matsuoka T, Maekawa Y, *et al.* Development of multicentric hepatocellular carcinoma after completion of interferon therapy. *J Gastroenterol* 2002; 37: 663–8.
16. Shindo M, Hamada K, Oda Y, *et al.* Long-term follow-up study of sustained biochemical responders with interferon therapy. *Hepatology* 2001; 33: 1299–302.
17. Ikeda M, Fujiyama S, Tanaka M, *et al.* Risk factors for development of hepatocellular carcinoma in patients with chronic hepatitis C after sustained response to interferon. *J Gastroenterol* 2005; 40: 148–56.
18. Toyoda H, Kumada T, Tokuda A, *et al.* Long-term follow-up of sustained responders to interferon therapy, in patients with chronic hepatitis C. *J Viral Hepatitis* 2000; 7: 414–9.
19. Makiyama A, Itoh Y, Kasahara A, *et al.* Characteristics of patients with chronic hepatitis C who develop hepatocellular carcinoma after a sustained response to interferon therapy. *Cancer* 2004; 101: 1616–22.
20. Tamori A, Nishiguchi S, Shiomi S, *et al.* Hepatitis B virus integration in hepatocellular carcinoma after interferon-induced disappearance of hepatitis C virus. *Am J Gastroenterol* 2005; 100: 1748–53.
21. Yoshida H, Arakawa Y, Sata M, *et al.* Interferon therapy prolonged life expectancy among chronic hepatitis C patients. *Gastroenterology* 2002; 123: 483–91.
22. Enokimura N, Shiraki K, Kawakita T, *et al.* Hepatocellular carcinoma development in sustained viral responders to interferon therapy in patients with chronic hepatitis C. *Anticancer Res* 2003; 23: 593–6.
23. Desmet VJ, Gerber M, Hoofnagle JH, *et al.* Classification of chronic hepatitis: diagnosis, grading and staging. *Hepatology* 1994; 19: 1513–20.
24. Manns MP, McHutchinson JG, Gordon SC, *et al.* Peginterferon alpha-2b plus ribavirin compared with interferon alpha-2b plus ribavirin for initial treatment of chronic hepatitis C: a randomised trial. *Lancet* 2001; 358: 958–65.
25. Fried MW, Shiffman ML, Reddy K, *et al.* Peginterferon alpha-2a plus ribavirin for chronic hepatitis C virus infection. *N Engl J Med* 2002; 347: 975–82.
26. Okita K. Clinical aspect of hepatocellular carcinoma in Japan. *Intern Med* 2006; 45: 229–33.
27. Larghi A, Tagger A, Crosignani A, *et al.* Clinical significance of HCV RNA in patients with chronic hepatitis C demonstrating long-term sustained response to interferon-alpha therapy. *J Med Virol* 1998; 55: 7–11.
28. Reichard O, Glaumann H, Fryden A, *et al.* Two-year biochemical, virological, and histological follow-up in patients with chronic hepatitis C responding in a sustained fashion to interferon alpha-2b treatment. *Hepatology* 1995; 21: 918–22.
29. Balart LA, Perrillo R, Roddenberry J, *et al.* Hepatitis C RNA in liver of chronic hepatitis C patients before and after interferon alpha treatment. *Gastroenterology* 1993; 104: 1472–7.
30. Hassan MM, Hwang LY, Hatten CJ, *et al.* Risk factors for hepatocellular carcinoma: synergism of alcohol with viral hepatitis and diabetes mellitus. *Hepatology* 2002; 36: 1206–13.
31. El-Serag HB, Richardson PA, Everhart JE. The role of diabetes in hepatocellular carcinoma: a case-control study among United States Veterans. *Am J Gastroenterol* 2001; 6: 2462–7.
32. Shimada M, Hashimoto E, Tanai M, *et al.* Hepatocellular carcinoma in patients with non-alcoholic steatohepatitis. *J Hepatol* 2002; 37: 154–60.
33. Ohta K, Hamasaki K, Toriyama K, *et al.* Hepatic steatosis is a risk factor for hepatocellular carcinoma in patients with chronic hepatitis C virus infection. *Cancer* 2003; 97: 3036–43.
34. Kiyosawa K, Uemura T, Ichijo T, *et al.* Hepatocellular carcinoma: recent trends in Japan. *Gastroenterology* 2004; 127: S17–26.

Available online at www.sciencedirect.com

Comparative Immunology, Microbiology
& Infectious Diseases ■ (■■■■) ■■■-■■■

C OMPARATIVE
I MMUNOLOGY
M ICROBIOLOGY &
I NFECTIONIOUS
D ISEASES

www.elsevier.com/locate/cimid

Comparative aspects on the role of polypyrimidine tract-binding protein in internal initiation of hepatitis C virus and picornavirus RNAs

T. Nishimura^{a,e}, M. Saito^a, T. Takano^{a,b,c}, A. Nomoto^d,
M. Kohara^b, K. Tsukiyama-Kohara^{a,b,c,*}

^aDepartment of Experimental Phylaxiology, Faculty of Medical and Pharmaceutical Sciences, Kumamoto University 1-1-1, Honjo, Kumamoto 860-8556, Japan

^bDepartment of Microbiology and Cell Biology, The Tokyo Metropolitan Institute of Medical Science, Tokyo 113-8613, Japan

^cLaboratory Animal Research Center, Institute of Medical Science, The University of Tokyo, Tokyo 108-8639, Japan

^dGraduate School of Medicine, The University of Tokyo, Tokyo 113-0033, Japan

^eThe Chemo-Sero-Therapeutic Research Institute, Tokyo 869-1298, Japan

Accepted 6 July 2007

Abstract

We compared the effects of polypyrimidine tract-binding protein (PTB) on hepatitis C virus (HCV genotype 1a), encephalomyocarditis virus (EMCV) and poliovirus internal ribosome entry site (IRES) activities *in vitro*. It bound strongly to EMCV IRES, but weakly to PV and HCV RNAs. PV IRES showed the strongest dependency to PTB and it showed less than one-tenth of IRES activity after the immuno-depletion of PTB from HeLa S10 lysate with pre-coated anti-PTB IgG beads, comparing to the normal IgG beads-treated S10 lysate. EMCV IRES activity was approximately 40% of that of normal control after PTB depletion.

*Corresponding author. Department of Experimental Phylaxiology, Faculty of Medical and Pharmaceutical Sciences, Kumamoto University 1-1-1, Honjo, Kumamoto 860-8556, Japan.
Tel./fax: +81 96 373 5560.

E-mail address: kkohara@kumamoto-u.ac.jp (K. Tsukiyama-Kohara).

0147-9571/\$ - see front matter © 2007 Elsevier Ltd. All rights reserved.

doi:10.1016/j.cimid.2007.07.002

Please cite this article as: Nishimura T, et al. Comparative aspects on the role of polypyrimidine tract-binding protein... *Comparat Immunol Microbiol Infect Dis.* (2007), doi:10.1016/j.cimid.2007.07.002

Especially, HCV IRES activity was approximately 95%, and most weakly affected by the depletion of PTB. Repletion of PTB to depleted S10 lysate restored activities of PV and EMCV IRESs. The data suggest that PTB plays an important role in picornaviral IRESs, but not in HCV IRES.

© 2007 Elsevier Ltd. All rights reserved.

Keywords: PTB; HCV; IRES; EMCV; PV; HeLa

Résumé

Dans notre étude, nous avons comparé les effets de la 'polypyrimidine track-binding' (PTB) virus de l'hépatite C (génotype IIa) et l'activité du virus encéphalomyéloblastite (EMCV) et de l'IRES du poliovirus *in vitro*. La PTB se fixe de manière résistante à l'IRES de l'EMCV mais de manière fragile à l'ARN du PV et du VHC. L'IRES du PV montre la dépendance la plus forte à la PTB et il montre une activité d'IRES de moins de un dixième après immunodéplétion de la PTB du lysat HeLa10 par des billes d'IgG anti-PTB prêtes à l'emploi, par rapport au HeLa10 traité par des billes d'IgG normales. L'activité de l'IRES de l'EMCV était approximativement égale à 40% de celle sous contrôle normal après déplétion de la PTB. L'activité de l'IRES du VHC était approximativement égale à 95% et la moins sensible à la déplétion de la PTB. La réplétion de la PTB au lysat S10 appauvri rétablit les activités des IRES du PV et de l'EMCV. Les données suggèrent que la PTB joue un rôle important dans les IRES picornaviraux mais pas dans les IRES du VHC. De plus,

© 2007 Elsevier Ltd. All rights reserved.

Mots clés: PTB; VHC; PTB; IRES; PV; HeLa

1. Introduction

Hepatitis C virus (HCV) possesses a single-stranded RNA (approximately 9610 nucleotides), and classified into the family *Flaviviridae* [1–4]. HCV is a major causative agent of non-A non-B hepatitis, and likely progresses into the chronic hepatitis, cirrhosis and hepatocellular carcinoma.

The 5' untranslated region (5'UTR) of HCV RNA genome is 341 nucleotides and an internal ribosome entry site (IRES) has been proven to exist in this region [5]. Activities of IRESs of HCV were different from each genotype, and genotype IIa showed almost two-fold higher IRES activity than genotype Ib [6,7].

The IRESs have been discovered in the *Picornavirus* genomes and have a complex RNA secondary structure [5,8]. The importance of secondary structure to IRES function is understood by studies that sequence substitutions within the IRES are accompanied by compensatory mutations that act to maintain the RNA secondary structure. The 40S ribosome subunit is recruited within these IRES without binding to the m⁷G cap and eIF4E [9,10]. IRESs can be classified into at least 3 groups, according to their features. IRESs derived from entero- and rhinoviruses are classified into type 1 (poliovirus), and oligopyrimidine tract is located in 50–100 nucleotides past the 3' end of the IRES [11,12]. The oligopyrimidine tract

immediately follows the 3' end of type 2 (cardio- and aphthoviruses) IRES. Encephalomyocarditis virus (EMCV) and foot and mouse disease virus possess type 2 IRESs and utilizes eIF4G and 4B [13,14]. The HCV and classical swine fever virus (CSFV) possess type 3 IRESs which interact directly to 40S ribosome subunit and eIF3 [15]. In addition to the requirement for eIF in each IRESs, the existence of internal initiation trans-acting factors (ITAFs) has been reported [16,17]. One of ITAFs binds to picornavirus and HCV IRES commonly is polypyrimidine tract-binding protein (PTB) [11,18–20]. PTB may work in each IRESs, however, its exact role in internal initiation has been still unclear at present. In the present study, requirement of PTB in poliovirus, EMCV and HCV IRESs has been characterized, and compared in *in vitro* translation system by depletion and complementation of PTB.

2. Materials and methods

2.1. Isolation of cDNA clones and construction of expression vectors

HCV cDNA that corresponds to nucleotide positions 1-418 (GenBank) was isolated by PCR from plasma of HCV type IIa infected patients [5], using a sense primer, 5'-GATCTAGAGCCCGCCCCCTGATGGGGGCGA-3', and antisense primer 5'-TGTCCTGCAGTTCAAGGGCCC-3'. The amplified cDNA was digested with XbaI and AatII, and replaced with an XbaI and AatII fragment (5'UTR) of pKIV [5]. A whole cDNA which was excised by XbaI-HindIII was filled up with Klenow fragment (Takara) and cloned into StuI site of pNar3 [5], and the resulting plasmid was designated as pNII5'.

Poliovirus cDNA expression vector T7M2, CAT gene with 5'UTR of EMCV (pBSECAT) and T7CAT were constructed, as described previously [19,21].

PTB cDNA that encodes whole coding region (amino acids no. 1-531) [22] or C terminal half (amino acids no. 291-531) of PTB was synthesized by RT-PCR, and cloned into the downstream of glutathione S transferase (GST) protein in frame in pGEX-KG vector, and was designated as pGST-PTB.

2.2. Expression of PTB and production of specific antibodies

The pGST-PTB was transformed in *Escherichia coli* strain SCS-1 and induced expression with 1 mM IPTG induction. *E. coli* culture (40 ml) was pelleted by centrifuge and lysed with lysozyme (1 mg/ml) and sonicated with 1% TritonX100 and 10 mM DTT. The supernatant was reacted to Glutathione Sepharose 4B (Amersham Bioscience), cleaved by thrombin (SIGMA) and purified with ploy U Sepharose 4B (Amersham Bioscience), as described previously [22]. Rabbits or guinea pigs immunized were over four times intradermal and subcutaneously or intraperitoneally with purified recombinant whole or C-terminal half of PTB (200 µg). These hyperimmune sera were purified by the protein G Sepharose 4B (Amersham Bioscience). The anti PTB rabbit IgG was further purified by the affinity

column of PTB cross-linking Formyl Cellulofine (Seikagaku Kogyo Co.), as described by manufacturer's instruction manual.

2.3. UV cross-linking assays and immunoprecipitation

RNA probes corresponding to nucleotide(nt.) 1-341 of the HCV 5'UTR, nt. 260-833 of the EMCV 5'UTR and nt. 1-747 of the PV 5'UTR were generated by the digestion of pNII5' with BspHI, pBSECAT with Ball and pM1(T7) with HgiAI, respectively, and transcribed by using Megascript™ T7 RNA polymerase kit (Ambion) with [α - 32 P]UTP (NEN). Labelled RNA probes were purified by the Nuc Trap™ push columns (Stratagene). Probes ($1-5 \times 10^6$ cpm) were incubated with or without competitor RNA in HeLa S10 lysate (10 μ g) at 30 °C for 20 min and irradiated on ice for 20 min in a UV Stratalinker (Stratagene). Unbound RNAs were digested with 10 μ g of RNase A (Sigma), 200 units of RNase T1 (Gibco BRL) and 1 unit of phosphodiesterase I (Amersham Bioscience). Samples were analyzed by SDS-PAGE and dried gel was exposed to imaging plate (Fuji) or X-ray film (Kodak). Radioactivity was measured by the Bio-image analyzer BAS 2000 (Fuji).

HeLa S10 or recombinant PTB which was UV cross-linked to labeled HCV RNA was solubilized by single lysis buffer containing 1% NP40, reacted with affinity-purified anti-PTB Ig (4 μ g) and precipitated by affigel protein A (Bio Rad) beads. Precipitated protein was further characterized by SDS-PAGE.

2.4. Immuno-depletion test

Affigel protein A (Bio Rad) 50 μ l was pretreated with HeLa S10 100 μ l at 37 °C for 1 h. The affinity purified anti-PTB Rabbit IgG (500 μ g) was added, and rotated at room temperature for 3 h. These IgG beads were coated by 10% FCS-0.1 M phosphate buffer (pH 8.0) at 37 °C for 1 h, washed with S10 dialysis buffer (10 mM Hepes-KOH pH7.5, 90 mM KOAc, 1.5 mM Mg(OAc) $_2$), and reacted to HeLa S10 lysate (150 μ l) at 4 °C overnight. The supernatants of each reaction were utilized for *in vitro* translation.

2.5. Competitive ELISA

Serocluster 'U' vinyl plate with 96 wells (Costar) was coated with affinity purified rabbit anti-PTB-C term IgG (2.5 μ g/ml) at 4 °C overnight. After blocking with 1% casein PBS (-) at 25 °C for 2 h, non-treated or immunodepleted HeLa S10 lysate were added to each well, and incubate at 25 °C for 2 h. Purified recombinant PTB was used for standard and non-treated or immunodepleted HeLa S10 lysates were added to each well, and incubate at 25 °C for 2 h. Then anti-PTB guinea pig IgG (1 μ g/ml) was reacted at 37 °C for 1 h, and finally anti-guineapig -IgG HRP (Dako 1:2000) was reacted at 37 °C for 1 h. *Ortho*-phenylene diamine was added to each well as substrate, and the absorbance was measured by microplate reader Model 450 (Bio Rad).

2.6. *In vitro* transcription and translation

Plasmids were linearized by digestion with XmnI (pNII5'), HpaI (pBSECAT) and NheI (p(M1)T7) and transcribed into RNA by Megascript™ T7 RNA polymerase kit (Ambion). RNAs were treated with DNase I, precipitated with LiCl, and quantitated by the Spectrophotometer DU64 (Beckman).

Synthetic RNAs (pNII5' RNA; 1.0 pmol, pBSECAT; 1.8 pmol, p(M1)T7; 0.36 pmol and they were optimized for the linear phase in translation activity) were translated in HeLa S10 lysates at 37 °C for 30 min with [³⁵S]-Methionine (ICN), as described previously [5]. Translation products were analyzed using 7.5–15% gradient SDS-PAGE.

2.7. Restoration assay

Purified recombinant PTB, bovine serum albumin and ribosome salt wash (RSW) were dialyzed to S10 dialysis buffer, and added to PTB depleted or non-treated HeLa S10. RSW (total 6.7 ml) was prepared from 6.11 of HeLa S10, as described previously [5] (kindly supplied by Dr. H. Toyoda).

3. Results

3.1. Fifty-seven and 60 kDa doublet protein bound HCV, EMCV and PV RNA

HeLa cytoplasmic proteins that were detected by UV cross-linking to ³²P-UTP labeled RNA derived from the HCV, EMCV, and PV 5'UTR were compared (Fig. 1). Total counts of binding proteins in HCV RNA was five times lower than those of EMCV RNA, and three times lower than those of PV-RNA (PSL; HCV 21536.9, EMCV 105622.8, PV 59307.9). Among these cytoplasmic proteins, 57 and 60 kDa doublet bands on HCV RNA, EMCV RNA and PV RNA have been identified to be PTB (Fig. 1, indicated by asterisk). According to band intensities of the 57 and 60 kDa proteins, PTB bound to EMCV IRES most abundantly, and more diminished amount of PTB bound to PV and HCV IRESs (Fig. 1).

3.2. Identification of P57/60 kDa doublet protein on HCV-RNA as PTB

HCV-IRES-binding proteins with molecular weight of 57/60 kDa were further characterized. The recombinant PTB protein was expressed in *E. coli* in the presence of IPTG, purified by glutathione sepharose and polyU sepharose column (Fig. 2A), and reacted with affinity purified anti-PTB IgG (Fig. 2B), as described in Section 2. Labeled HCV RNA 5'UTR was cross-linked to HeLa S10 lysate, and immunoprecipitated by affinity purified anti-PTB IgG (Fig. 3). The 57 and 60 kDa doublet bands were specifically reacted to the anti-PTB IgG (Fig. 3, lane HeLa). The recombinant PTB protein was cross-linked with HCV RNA 5'UTR and precipitated with anti-PTB IgG (Fig. 3, lane PTB). These results strongly indicate that PTB

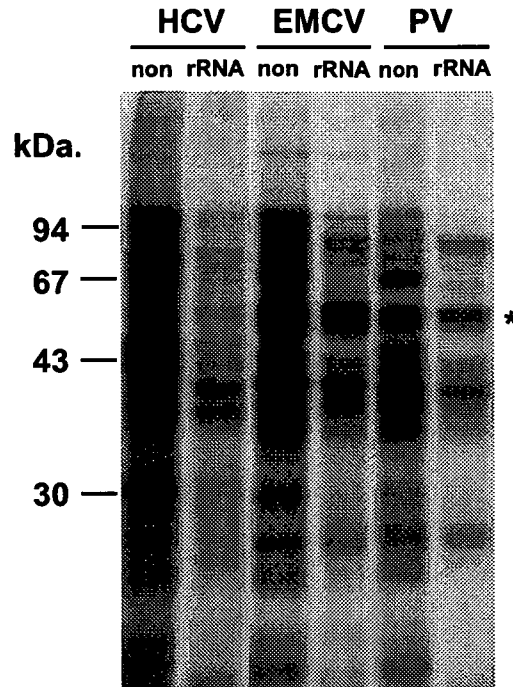


Fig. 1. UV-cross-linking analysis of binding factors to HCV, EMCV and PV-IRES RNAs. Each reaction without competitor indicates "non", and with competitor rRNA indicates rRNA on the top of the lanes. Asterisk indicates the position of PTB proteins. An asterisk indicates PTB binding.

specifically bound to HCV RNA 5'UTR, and observed as doublet protein with molecular weight of 57 and 60 kDa.

3.3. Depletion of PTB in HeLa S10 lysate

Previous results indicated the possibility that other factors than canonical eukaryotic translation initiation factors (eIFs) are working in cap independent translation. PTB is one of the candidates and when the PTB might be commonly used in several kinds of IRESs, it might play the central role in internal initiation. To compare the significance of PTB in translation initiation in HCV and other Picorna virus IRESs, PTB in HeLa S10 lysate was depleted by affinity purified anti-PTB IgG. For the depletion of PTB, pre-coating of Affi-gel protein A beads was necessary to block the non-specific adsorption, as described in Section 2. Pre-coated beads were reacted with anti-PTB IgG. From the preliminary experiments, more than 100 times higher molar ratio of anti-PTB IgG to PTB in S10 lysates was required for the over 90% depletion, as described in Materials and methods. We performed the PTB depletion, and 94.5% of PTB was depleted by anti-PTB IgG and 26.3% of PTB was depleted by pre-immune IgG (Fig. 4). We further examined the effect of PTB

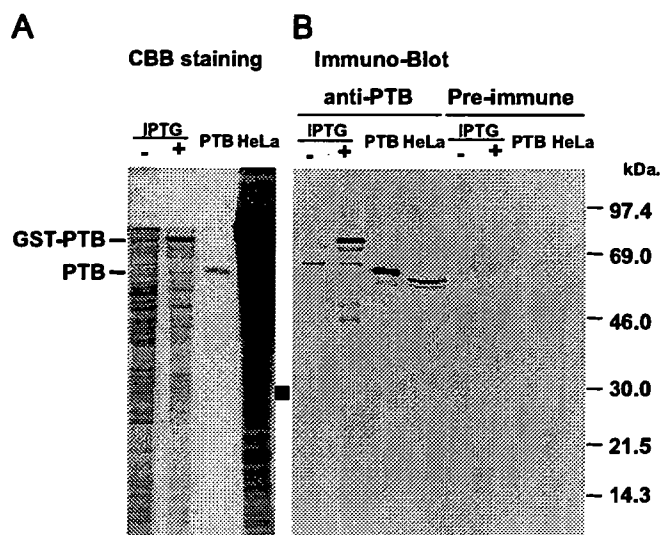


Fig. 2. Expression of recombinant PTB protein fused with GST in *E. coli*: (A) Expression of PTB protein was induced by IPTG, purified by glutathione sepharose column and stained with CBB. (B) Expressed recombinant PTB was transferred to membrane and reacted with specific antibody by WB.

depletion to the binding of cellular factors to three IRESs (Fig. 5). In PTB depleted lysates, binding of 57 and 60 kDa doublet protein was decreased, especially in PV-RNA. However, binding of other factors was not influenced significantly, other than 28 kDa protein (Fig. 5, indicated by an arrow).

3.4. Effect of PTB depletion in translation

Influence of PTB depletion was examined in HCV, EMCV and PV-RNA (Fig. 6A, Table 1). The reaction curves of each RNA were different from each other (data not shown), and the optimum quantity of each RNA used in this study was different from each other (Table 1). From the comparison of translation activity in PTB depleted S10 lysates, translation of PV-RNA was significantly decreased in 4 and 8 μ l lysates (22–4.5%, 15–0.9%, Table 1, Fig. 6A). Translation of EMCV-IRES was significantly decreased after PTB depletion (53–44% (4 μ l), 28–11% (8 μ l)), but this suppression was not as much as PV-IRES. Activity of HCV-IRES was almost similar between pre-immune IgG-treated and anti-PTB IgG-treated S10 lysates. Because the optimal RNA quantities for translation are different in each IRESs, therefore, we calculated the ratio of PTB quantity per template RNA molecules (PTB/RNA) (ng/pmol; Table 1). In PV-IRES, translation activity was significantly reduced after depletion (4.5%, 0.9%) and the PTB/RNA ratio was 1.4 and 0.56. EMCV-IRES and HCV-IRES activity. Influence of PTB depletion to HCV-IRES activity was much lower than those of PV and EMCV.

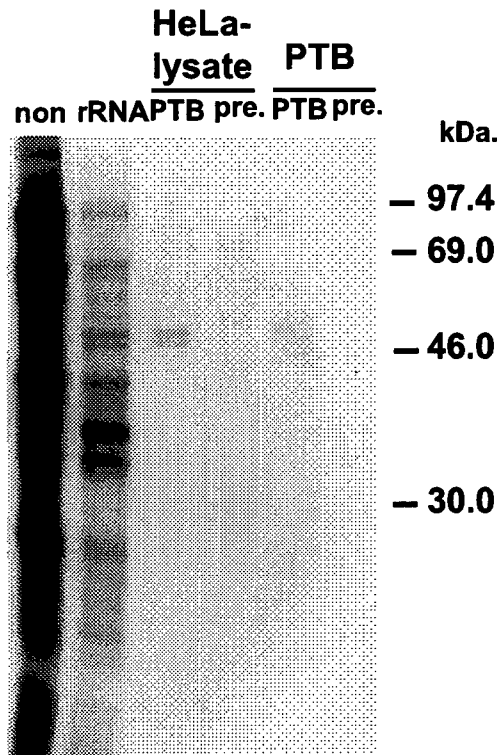


Fig. 3. HCV-IRES cross-linked S10 and PTB was immuno-precipitated by purified anti PTB antibody and pre-immune antibody. The 57 and 60 kDa doublet bands were specifically reacted to the anti-PTB IgG (lane HeLa). The recombinant PTB protein was cross-linked with HCV RNA 5'UTR and precipitated with anti-PTB IgG (lane PTB). Pre-immune antibody did not reacted to both Hela S10 and PTB.

The IRES activity of EMCV and PV-RNA was decreased by treatment of pre-immune IgG, however, treatment of pre-immune IgG did not influence significantly to the IRES activity of HCV-RNA.

3.5. Restoration of PTB to depleted S10

To clarify the effect of immuno-depletion was mainly caused by the decreased quantity of PTB, the purified recombinant PTB or RSW was added to depleted S10 (Fig. 6B). The IRES activity of PV-RNA in depleted S10 lysate (6 μ l) was increased by the addition of PTB in dose-dependent manner. The EMCV-IRES activity was recovered even in the presence of 1 μ g of PTB in depleted S10 lysate (4.0 μ l). When too much quantity of PTB was added to the S10, translation activity of PV, EMCV and HCV decreased (over 10 times of PTB in PV, over 300 times in EMCV and over 500 times in HCV RNA, data not shown).

Translation activity of PV and EMCV-RNA became higher after the addition of RSW to anti-PTB IgG depleted S10 (150% and 117%, respectively) (date not

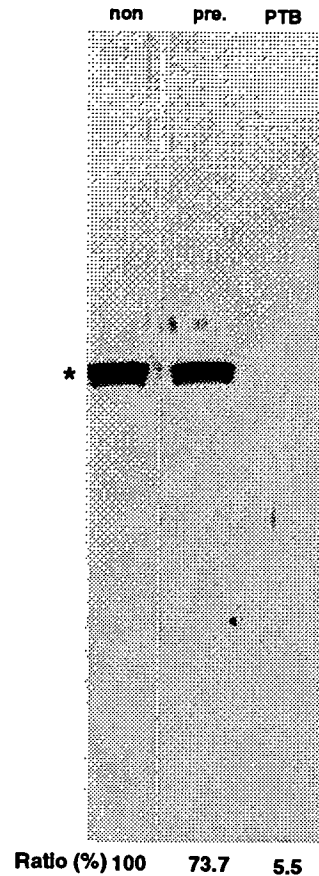


Fig. 4. Depletion of HeLa S10 by pre-immune IgG and affinity purified anti-PTB IgG. They were reacted with anti-PTB antibody by WB. Asterisk indicates the position of PTB proteins. Anti-PTB IgG deplete 94.5% of PTB (lane PTB) and pre-immune IgG deplete 26.3% of PTB (lane pre).

shown). This might indicate the existence of several translation factors other than PTB, which were lost during the treatment of IgG.

Taken together, results of this study strongly indicate that significance of PTB was highest in PV-IRES and was lowest implication in HCV-IRES.

4. Discussion

In present study, the significance of PTB in HCV, EMCV and PV IRESs has been compared. From the immuno-depletion experiment (Table 1), PTB-Ig depleted S10 (4.0 μ l) contained 0.009 molecule of PTB per 1 molecule of RNA, in which PV IRES activity is 0.9%. This may indicate that almost one PTB molecule should be required

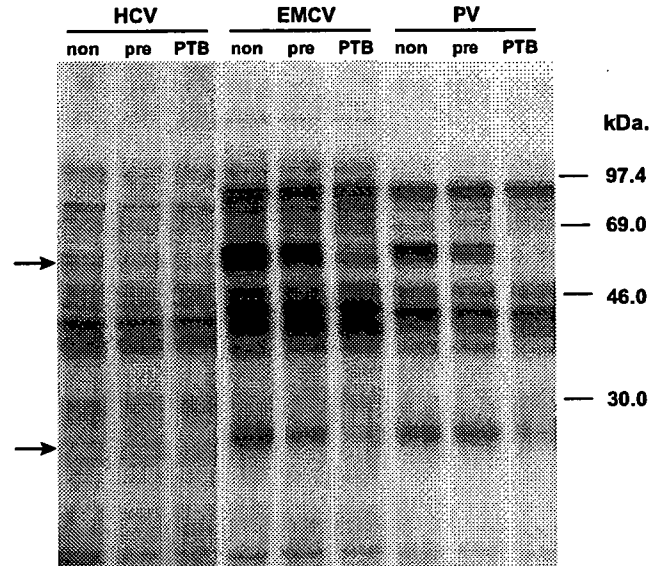


Fig. 5. UV-cross-linking analysis of HCV, EMCV and PV RNA with non-treated, pre-immune IgG-treated, and anti-PTB IgG-treated HeLa S10 lysate (lane non, pre, PTB). Upper arrow indicates the binding of PTB. Doublet protein (57 and 60 kDa) was decreased, especially in PV-RNA. Lower arrow indicates 28 kDa protein.

for 100% activity of PV IRES-RNA. In the case of EMCV IRES-RNA, 0.002 molecule of PTB per RNA gave 11% of EMCV IRES activity, and that of HCV IRES, 0.0025 molecule of PTB gave 31% of HCV IRES activity. Therefore, requirement of PTB for IRES activity was highest in PV, and less in EMCV and HCV IRES-RNA.

From the results in this study, we can compare the requirement amount of PTB in IRES activity with those of canonical eIFs. The most limiting initiation factor in cells is eIF4E, with estimates in rabbit reticulocyte lysates ranging from 0.02 copies [23] to 1 copy [24] per ribosome. The concentration of ribosomes has been estimated to be approximately 2 μ M [25]. From the results of *in vitro* translation experiment, PTB should work at 0.1–0.15 M in each IRESs at maximum activity (Table 1). Therefore, working concentration of PTB for IRES activity should show almost similar to those of eIFs.

During the immuno-depletion experiment, treatment of normal IgG conjugated beads decreased the IRESs activity; 89 (6.5 μ l) or 33 (3.5 μ l)% in HCV IRES, 53 or 28% in EMCV IRES, and 22% or 15% in PV-IRES (Table 1). This may suggest the existence of unknown factors, which could be inactivated during the process of immuno-depletion experiment, and these effects in PV-IRES were highest among the IRESs. PV-IRES is classified into the type I [26], and the canonical eIFs with the exception of cap-binding protein eIF4E [27] and PTB [26], La [26] and 39 kDa poly(rC)-binding protein [26] are working. In EMCV IRES (type II), eIF4G was

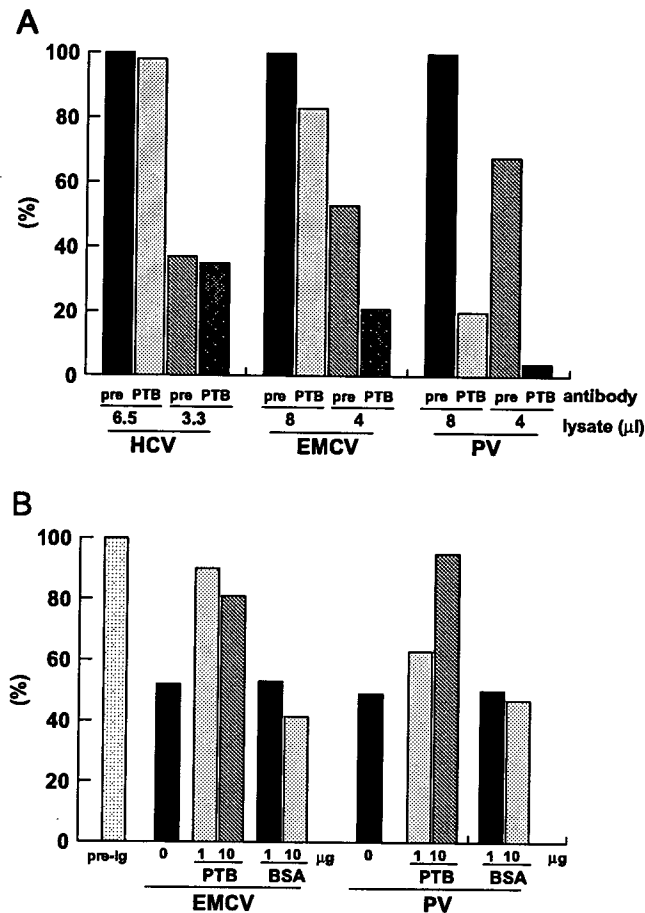


Fig. 6. (A) Effect of PTB depletion in HCV, EMCV and PV IRES. IRESs were translated in pre-immune IgG-depleted and anti-PTB IgG depleted S10 lysates (3.3, 6.5 μl in HCV-IRES, 4.0, 8.0 μl in EMCV- and PV-IRES. Translated products in SDS-PAGE were measured by image analyzer, and the quantity (PSL) of pre-immune IgG-treated S10 lysate was calculated as 100%. (B) Recovery of translation in PTB depleted S10 lysate by addition of recombinant PTB protein (1 and 10 μg. Translated products in SDS-PAGE were measured by image analyzer, and the quantity (PSL) of pre-immune IgG-treated S10 lysate was calculated as 100%.

directly bound and eIF4A and eIF4B can recruit 43S preinitiation complex which is composed of 40S ribosomal subunit and eIF3, eIF2, GTP and initiator tRNA[13]. Recent findings indicated the dependence of EMCV IRES on PTB for activity [28]. The HCV IRES possesses striking difference from type I and II IRESs, it recruits 43S preinitiation complex to initiation codon to form a 48S complex without involvement of eIF4A, 4B or 4F [29]. Thus, HCV IRES is simple and does not require most of eIFs, and might not be influenced by the depletion experiment using normal IgGs.

Table 1
Effect of PTB depletion in HCV, EMCV and PV IRES

RNA	RNA quantity (pmol)	S10 (μl)	PTB (ng)	Molar ratio of PTB to RNA	Ratio of translation (%) ^a	
HCV	1.0	<i>Untreated</i>				
		6.5	7.2	0.12	100	
		3.5	3.6	0.06	63	
		<i>Pre-im.-IgG</i>				
		6.5	5.2	0.085	89	
		3.5	2.6	0.045	33	
		<i>αPTB-IgG</i>				
		6.5	0.4	0.005	87	
		3.5	0.2	0.0025	31	
EMCV	1.8	<i>Untreated</i>				
		8.0	8.8	0.08	100	
		4.0	4.4	0.04	57	
		<i>Pre-im.-IgG</i>				
		8.0	6.4	0.06	53	
		4.0	3.2	0.03	28	
		<i>αPTB-IgG</i>				
		8.0	0.5	0.005	44	
		4.0	0.2	0.002	11	
PV	0.36	<i>Untreated</i>				
		8.0	8.8	0.4	100	
		4.0	4.4	0.2	65	
		<i>Pre-im.-IgG</i>				
		8.0	6.4	0.3	22	
		4.0	3.2	0.15	15	
		<i>αPTB-IgG</i>				
		8.0	0.5	0.02	4.5	
		4.0	0.2	0.009	0.9	

^aRatio of translation products was quantitated by image analyzer.

Recent riboproteomic approach revealed the novel interacting proteins to IRESs [30], other than PTB, such as actin, forming homolog overexpressed in spleen, and microtubule interacting protein that associates with TRAF3. These factors should be characterized as novel ITAFs and comparative aspects in different IRESs should be addressed in the future work to clarify the character of each IRESs.

Acknowledgments

This work was supported by the grants from the Ministry of Health and Welfare, or Education, Culture, Sports, Science and Technology of Japan, the program for

promotion of fundamental studies in health sciences of the National Institute of Biomedical Innovation, and the Cooperative Research Project on Clinical and Epidemiological Studies of Emerging and Re-emerging Infectious Diseases.

References

- [1] Choo QL, Kuo G, Weiner AJ, Overby LR, Bradley DW, Houghton M. Isolation of a cDNA clone derived from a blood-borne non-A, non-B viral hepatitis genome. *Science* 1989;244:359–62.
- [2] Takamizawa A, Mori C, Fuke I, Manabe S, Murakami S, Fujita J, et al. Structure and organization of the hepatitis C virus genome isolated from human carriers. *J Virol* 1991;65:1105–13.
- [3] Kato N, Hijikata M, Ootsuyama Y, Nakagawa M, Ohkoshi S, Sugimura T, et al. Molecular cloning of the human hepatitis C virus genome from Japanese patients with non-A, non-B hepatitis. *Proc Natl Acad Sci USA* 1990;87:9524–8.
- [4] Kaito M, Watanabe S, Tsukiyama-Kohara K, Yamaguchi K, Kobayashi Y, Konishi M, et al. Hepatitis C virus particle detected by immunoelectron microscopic study. *J Gen Virol* 1994;75(Part 7):1755–60.
- [5] Tsukiyama-Kohara K, Iizuka N, Kohara M, Nomota A. Internal ribosome entry site within hepatitis C virus RNA. *J Virol* 1992;66:1476–83.
- [6] Kamoshita N, Tsukiyama-Kohara K, Kohara M, Nomoto A. Genetic analysis of internal ribosomal entry site on hepatitis C virus RNA: implication for involvement of the highly ordered structure and cell type-specific transacting factors. *Virology* 1997;233:9–18.
- [7] Nomoto A, Tsukiyama-Kohara K, Kohara M. Mechanism of translation initiation on hepatitis C virus RNA. *Princess Takamatsu Symp* 1995;25:111–9.
- [8] Pelletier J, Sonenberg N. Internal initiation of translation of eukaryotic mRNA directed by a sequence derived from poliovirus RNA. *Nature* 1988;334:320–5.
- [9] Kieft JS, Zhou K, Jubin R, Doudna JA. Mechanism of ribosome recruitment by hepatitis C IRES RNA. *RNA* 2001;7:194–206.
- [10] Yu Y, Ji H, Doudna JA, Leary JA. Mass spectrometric analysis of the human 40S ribosomal subunit: native and HCV IRES-bound complexes. *Protein Sci* 2005;14:1438–46.
- [11] Hellen CU, Pestova TV, Litterst M, Wimmer E. The cellular polypeptide p57 (pyrimidine tract-binding protein) binds to multiple sites in the poliovirus 5' nontranslated region. *J Virol* 1994;68:941–50.
- [12] Hunt SL, Jackson RJ. Polypyrimidine-tract binding protein (PTB) is necessary, but not sufficient, for efficient internal initiation of translation of human rhinovirus-2 RNA. *RNA* 1999;5:344–59.
- [13] Kolupaeva VG, Pestova TV, Hellen CU, Shatsky IN. Translation eukaryotic initiation factor 4G recognizes a specific structural element within the internal ribosome entry site of encephalomyocarditis virus RNA. *J Biol Chem* 1998;273:18599–604.
- [14] Kolupaeva VG, Hellen CU, Shatsky IN. Structural analysis of the interaction of the pyrimidine tract-binding protein with the internal ribosomal entry site of encephalomyocarditis virus and foot-and-mouth disease virus RNAs. *RNA* 1996;2:1199–212.
- [15] Sizova DV, Kolupaeva VG, Pestova TV, Shatsky IN, Hellen CU. Specific interaction of eukaryotic translation initiation factor 3 with the 5' nontranslated regions of hepatitis C virus and classical swine fever virus RNAs. *J Virol* 1998;72:4775–82.
- [16] Witherell GW, Wimmer E. Encephalomyocarditis virus internal ribosomal entry site RNA-protein interactions. *J Virol* 1994;68:3183–92.
- [17] Schepers GC, Voorma HO, Thomas AA. Binding of eukaryotic initiation factor-2 and trans-acting factors to the 5' untranslated region of encephalomyocarditis virus RNA. *Biochimie* 1994;76:801–9.
- [18] Ali N, Siddiqui A. Interaction of polypyrimidine tract-binding protein with the 5' noncoding region of the hepatitis C virus RNA genome and its functional requirement in internal initiation of translation. *J Virol* 1995;69:6367–75.
- [19] Jang SK, Wimmer E. Cap-independent translation of encephalomyocarditis virus RNA: structural elements of the internal ribosomal entry site and involvement of a cellular 57-kDa RNA-binding protein. *Genes Dev* 1990;4:1560–72.

- [20] Luz N, Beck E. Interaction of a cellular 57-kDa protein with the internal translation initiation site of foot-and-mouth disease virus. *J Virol* 1991;65:6486–94.
- [21] Jang SK, Pestova TV, Hellen CU, Witherell GW, Wimmer E. Cap-independent translation of picornavirus RNAs: structure and function of the internal ribosomal entry site. *Enzyme* 1990;44:292–309.
- [22] Garcia-Blanco MA, Jamison SF, Sharp PA. Identification and purification of a 62,000-Da protein that binds specifically to the polypyrimidine tract of introns. *Genes Dev* 1989;3:1874–86.
- [23] Hiremath LS, Webb NR, Rhoads RE. Immunological detection of the messenger RNA cap-binding protein. *J Biol Chem* 1985;260:7843–9.
- [24] Rau M, Ohlmann T, Morley SJ, Pain VM. A reevaluation of the cap-binding protein, eIF4E, as a rate-limiting factor for initiation of translation in reticulocyte lysate. *J Biol Chem* 1996;271:8983–90.
- [25] Duncan R, Hershey JW. Identification and quantitation of levels of protein synthesis initiation factors in crude HeLa cell lysates by two-dimensional polyacrylamide gel electrophoresis. *J Biol Chem* 1983;258:7228–35.
- [26] Flint SJ, Enquist LW, Krug RM, Racaniello VR, Skalka AM, editors. *Virology*. Washington, DC: ASM Press; 2000.
- [27] Gingras AC, Svitkin Y, Belsham GJ, Pause A, Sonenberg N. Activation of the translational suppressor 4E-BP1 following infection with encephalomyocarditis virus and poliovirus. *Proc Natl Acad Sci USA* 1996;93:5578–83.
- [28] Kaminski A, Jackson RJ. The polypyrimidine tract binding protein (PTB) requirement for internal initiation of translation of cardiovirus RNAs is conditional rather than absolute. *RNA* 1998;4:626–38.
- [29] Hellen CU, Pestova TV. Translation of hepatitis C virus RNA. *J Viral Hepat* 1999;6:79–87.
- [30] Lu H, Li W, Noble WS, Payan D, Anderson DC. Riboproteomics of the hepatitis C virus internal ribosomal entry site. *J Proteome Res* 2004;3:949–57.

Adipose Tissue-Derived Mesenchymal Stem Cells as a Source of Human Hepatocytes

Agnieszka Banas,¹ Takumi Teratani,¹ Yusuke Yamamoto,^{1,2} Makoto Tokuhara,³ Fumitaka Takeshita,¹ Gary Quinn,^{1,4} Hitoshi Okochi,³ and Takahiro Ochiya¹

Recent observations indicate that several stem cells can differentiate into hepatocytes; thus, cell-based therapy is a potential alternative to liver transplantation. The goal of the present study was to examine the *in vitro* hepatic differentiation potential of adipose tissue-derived mesenchymal stem cells (AT-MSCs). We used AT-MSCs from different age patients and found that, after incubation with specific growth factors (hepatocyte growth factor [HGF], fibroblast growth factor [FGF1], FGF4) the CD105⁺ fraction of AT-MSCs exhibited high hepatic differentiation ability in an adherent monoculture condition. CD105⁺ AT-MSC-derived hepatocyte-like cells revealed several liver-specific markers and functions, such as albumin production, low-density lipoprotein uptake, and ammonia detoxification. More importantly, CD105⁺ AT-MSC-derived hepatocyte-like cells, after transplantation into mice incorporated into the parenchyma of the liver. **Conclusion:** Adipose tissue is a source of multipotent stem cells that can be easily isolated, selected, and induced into mature, transplantable hepatocytes. The fact that they are easy to procure *ex vivo* in large numbers makes them an attractive tool for clinical studies in the context of establishing an alternative therapy for liver dysfunction. (HEPATOLOGY 2007;46:219-228.)

Regenerative medicine holds promise for the development of stem-cell-based therapy of the liver and may allow transplanting hepatocytes or liver devices generated *in vitro* from stem cells. The establish-

ment of stem cell therapy requires multipotential, immunocompatible stem cells and a direct differentiation strategy, that is not followed by post-transplantation complications or unwanted differentiation such as tumor formation. Many types of stem cells from different sources have been investigated for hepatic differentiation ability; mostly mouse, but also monkey and human embryonic stem (ES) cells have been used.¹ We have established the direct differentiation of mouse ES cells into functional hepatocytes in an adherent monoculture condition by the use of the HIFC method.^{2,3} In our method, growth factors directing hepatic fate specification have been identified on the basis of an *in vivo* transplantation of ES cells into liver-injured animals.⁴

ES cells have enormous potential; however, many limitations, such as teratoma formation followed by tumor genesis, immunogenicity, and ethical issues, are arresting their clinical usage. Adult human stem cells are promising candidates for liver regeneration,⁵⁻¹⁰ and their usage might sidestep obstacles, such as ethical concerns and risks of rejection. Currently, the focus is on mesenchymal stem cells (MSCs), found in human bone marrow (BM),¹¹ adipose tissue (AT),^{12,13} scalp tissue,¹⁴ placenta,¹⁵ and umbilical cord blood (UCB)¹⁶ as well as in various fetal tissues.¹⁷ These stem cells can differentiate *in vitro* into multiple types of lineages such as: chondrogenic, osteogenic, adipogenic,¹¹ myogenic,¹⁸

Abbreviations: ES, embryonic stem; HIFC, hepatic induction factor cocktail; HGF, hepatocyte growth factor; FGF, fibroblast growth factor; MSC, mesenchymal stem cell; BM, bone marrow; AT, adipose tissue; PBS, phosphate-buffered saline; DMEM, Dulbecco's modified Eagle medium; FBS, fetal bovine serum; EDTA, ethylenediaminetetraacetic acid; TGF, transforming growth factor; MACS, magnetically activated cell-sorting; HCM, hepatocyte culture medium; OsM, oncostatin M; TTR, transthyretin; ALB, albumin; TDO2, tryptophan 2,3-dioxygenase; AFP, alpha-fetoprotein; CK, cytokeratin; HNF, hepatocyte nuclear factor; LDL, low-density lipoprotein; PAS, periodic acid-Schiff; GPT, glutamic-pyruvic transaminase; FITC, fluorescein isothiocyanate; CD, cluster of differentiation antigen.

From the ¹Section for Studies on Metastasis, National Cancer Center Research Institute 1-1, Tokyo, Japan; ²Department of Biology, School of Education, Waseda University, Nishi-Waseda, Tokyo, Japan; ³Department of Surgery, International Medical Center of Japan, Tokyo, Japan; and ⁴Effector Cell Institute, Inc., Tokyo, Japan.

Received August 17, 2006; accepted February 21, 2007.

Supported in part by a Grant-in-Aid for the Third-Term Comprehensive 10-Year Strategy for Cancer Control; Health Science Research Grants for Research on the Human Genome and Regenerative Medicine from the Ministry of Health, Labor, and Welfare of Japan; and a Grant for Japan Health Sciences Foundation.

Address reprint requests to: Takahiro Ochiya, Ph.D., Head of Section for Studies on Metastasis, National Cancer Center Research Institute, 1-1, Tsukiji 5-chome, Chuo-ku, Tokyo 104-0045, Japan. E-mail: tochiya@ncc.go.jp; fax: (81) 3-3541-2685.

Copyright © 2007 by the American Association for the Study of Liver Diseases.

Published online in Wiley InterScience (www.interscience.wiley.com).

DOI 10.1002/hep.21704

Potential conflict of interest: Nothing to report

Supplementary material for this article can be found on the HEPATOLOGY website (<http://interscience.wiley.com/jpages/0270-9139/suppmat/index.html>).

Table 1. Adipose Tissue Donor Information

Donor (n)	Age (Years)	Gender	Height (cm)	Weight (kg)	BMI (kg/m ²)	Comments
1	54	male	158	61.7	24.7	gastric cancer
2	45	male	180	86.2	26.6	gastric cancer
3	43	female	165	62.0	22.8	gastric cancer
4	55	male	164	67.3	25.0	gastric cancer
5	45	female	149	47.2	21.5	gastric cancer
6	36	female	160	42.0	16.4	gastric cancer

NOTE. Adipose tissue was harvested from 6 cancer patients (three males, three females), undergoing gastrectomy. Patients' parameters such as: BMI, body mass, height, disease are of similar category.

neurogenic¹⁹ and hepatogenic,⁷⁻¹⁰ depending on the microenvironment in which they reside. MSCs from BM and UCB have been induced into a hepatic lineage⁷⁻¹⁰; however, the question of whether these are the best sources of stem cells for hepatic replacement and/or regeneration remains. Adipose tissue is an attractive source of multipotent human MSCs. AT-MSCs, so-called processed lipoaspirate (PLA) cells,^{12,13,20} adipose-derived stromal cells (ADSCs),²¹ adipose-derived adherent stromal cells/adipose-derived adult stem cells (ADASs),²²⁻²⁴ and adipose tissue-derived stromal cells (ATSCs)²⁵ are considered to be the multipotent fraction of adherent cells, which, after isolation of the adipose stromal vascular fraction (SVF), attach to plastic culture dishes and remain there as a heterogeneous population of fibroblast-like cells. AT-MSCs are very similar to BM-MSCs.^{20,26} Besides the fact that they are more heterogeneous²⁵, they reveal a surface antigen marker profile^{22,26-28} and differentiation potential similar to BM-MSCs.^{21,29-33} AT-MSCs are characterized as CD45⁻ CD34⁺ CD105⁺ CD31⁻³⁴; however, there is confusion regarding the CD34 marker. One of the markers defining MSC provenance is CD105 (endoglin).^{11,35,36} CD105 is a component of the receptor complex of transforming growth factor (TGF)-beta, a pleiotropic cytokine involved in cellular proliferation, differentiation, and migration. CD105⁺ cells from bone marrow displayed more colony-forming unit-fibroblasts (CFU-Fs) and revealed a capacity to form bone *in vivo*³⁷ and differentiate into a chondrogenic lineage.³⁸ The adipogenic and myogenic differentiation ratio of CD105⁺ BM-MSCs was not influenced by the age of the donor; however, the ratio usually decreased in older patients.³⁹ The ratio of the number of CD105⁺ stem cells in adipose tissue to the age of the donor is not clear, and little is known about the relationship between disease (e.g., cancer) and stem cell potential.

The aim of our present study was to evaluate the hepatogenic potential of AT-MSCs. Because therapy concerns patients, not healthy donors, we have used AT-MSCs from non-obese cancer patients undergoing gastrectomy. We performed magnetically activated cell-

sorting (MACS) of the CD105 fraction in order to achieve a multipotent and homogeneous subpopulation of cells. CD105⁺ AT-MSCs were highly inducible into the hepatic lineage, and derived hepatocyte-like cells expressed the liver markers, proteins, enzymes, and functions of human primary hepatocytes. The differentiation potential of AT-MSCs that we have advanced by *in vivo* transplantation into immunodeficient mice resulted in incorporation of AT-MSC-derived hepatocytes into the CCl₄-injured liver. Thus, human AT-MSCs, which might be obtained in a large number of cells, represent a very attractive tool for future stem cell therapy of the liver diseases.

Materials and Methods

Isolation and Culturing of AT-MSCs. Abdominal subcutaneous adipose tissue was obtained from six gastric cancer patients undergoing gastrectomy at the International Medical Center of Japan in Tokyo. All patients (Table 1) (age: 36-55 years old; mean: 46) exhibited comparable features (body weight, height, BMI, gastric cancer). The hospital's committee of ethics approved this study, and informed consent was obtained from all patients. Adipose tissue was minced with scissors and scalpels into less than 3-mm pieces and isolation of AT-MSCs proceeded as previously described.^{12,13} Briefly, after gentle shaking with equal volume of PBS(-), the mixture have separated into two phases. The upper phase (containing stem cells, adipocytes and blood) after washing with phosphate-buffered saline (PBS) (-) was enzymatically dissociated with 0.075% collagenase (type I)/PBS(-) for 1 hour at 37°C with gentle shaking. The dissociated tissue was then mixed with an equal volume of DMEM (GIBCO-BRL, Tokyo, Japan) supplemented with 10% fetal bovine serum (FBS) and incubated 10 minutes at room temperature. The solution then was separated into two phases. The lower phase was centrifuged at 1,500rpm for 5 minutes at 20°C. The cellular pellet was resuspended in 160mM NH₄Cl to eliminate erythrocytes

and passed through a 40 μ m mesh filter into a new tube. The cells were resuspended in an equal volume of DMEM/10% FBS and then centrifuged. Isolation resulted in obtaining $\approx 7.7 \times 10^6$ of adherent cells for a primary culture from 5g of adipose tissue (approximately; 1.0×10^5 to 4.6×10^6 /1g) (Fig. 1A, step I) after 7-10 days of culture. The cells were suspended in a DMEM/10% FBS plated in concentration $1-5 \times 10^6$ cells/75cm². The cells with 70%-80% confluence were harvested with 0.25% trypsin-EDTA and then either re-plated at 1.0×10^5 cells/60-mm dish and used for analysis or sorted using MACS system (Miltenyi Biotec., Bergisch Gladbach, Germany) (Fig. 1A, step II). Representative samples of each cell population were evaluated for hepatic and adipogenic differentiation capacity.

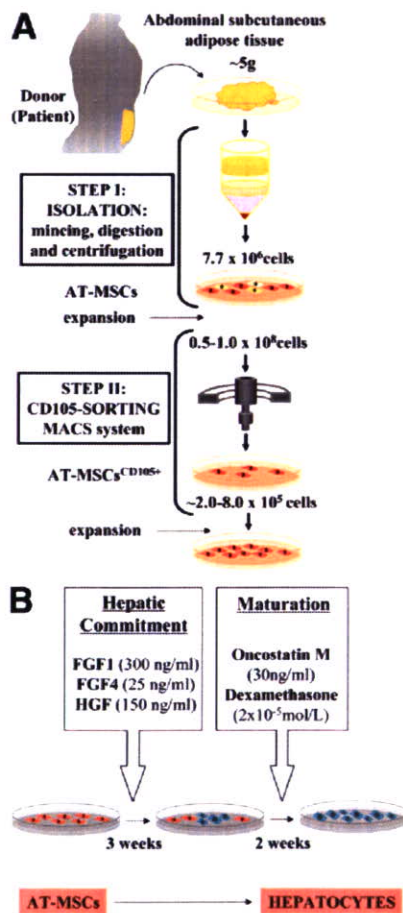


Fig. 1. Experimental strategy. A schematic representation of isolation (Step I), sorting (Step II) (A) and hepatic differentiation (B) of AT-MSCs. AT-MSCs after mincing, digestion with collagenase and centrifugation have been sorted by the MACS system. After expansion, CD105⁺ AT-MSCs were replated into type I collagen-coated dishes and differentiated into hepatocytes (B). Cells were treated for 3 weeks with a hepatic induction growth factor cocktail (HIFC), followed by 2 weeks of culturing with OsM/dexamethasone, and finally maintained in HCM for 2-5 weeks.

Isolation of the CD105⁺ Fraction from AT-MSCs.

The CD105⁺ fraction was isolated from AT-MSCs of three donors using CD105-coupled magnetic microbeads (Miltenyi Biotec) (Fig. 1A, Step II). Briefly, trypsinized AT-MSCs (passage 3-8; $0.5-1.0 \times 10^8$ cells) were suspended in a MACS buffer (PBS/0.5 bovine serum albumin/2mM EDTA) and incubated with antibodies (8°C, 15 minutes). After rinsing with the MACS buffer and centrifugation ($200 \times g$, 10 minutes), the cells were separated on a magnetic column. After the separation, approximately $2.0-8.0 \times 10^5$ CD105⁺ cells were achieved, plated in 60mm dishes, expanded, and used for experimental analysis.

Flow Cytometry. The phenotype of AT-MSCs was evaluated by flow cytometry analysis (FACS, Epic XL, Software Expo 32 (Beckman coulter)), by using CD29 (BD Bioscience Pharmingen, Tokyo, Japan), CD31, CD45 (eBioscience, Tokyo, Japan), CD34 (DacoCytomation, Carpinteria, USA) and CD105 (Ancell, Bayport, MN, USA) antibodies, coupled to either phycoerythrin (PE) or fluorescein isothiocyanate (FITC).

In vitro Cultivation and Expansion of BM-MSC, BM-HSC, and HepG2 Cells. Human BM-MSCs and hematopoietic CD34⁺ stem cells (BM-HSCs) (Cambrex Corp., Walkersville, MD) were cultured subsequently in a mesenchymal stem cell-growth medium (MSC-GM) and a serum-free Hematopoietic Progenitor Growth Medium (HPGM) (Cambrex). HepG2 cells were cultured in type I collagen-coated dishes under the same conditions as AT-MSCs. Human cryopreserved primary hepatocytes were obtained from TaKaRa (Kyoto, Japan) and cultured in Hepatic Culture Medium (HCM) (Cambrex).

Hepatic Differentiation by HIFC Method. At passage 5-9, $2-3 \times 10^5$ CD105⁺ AT-MSCs were plated onto 60mm collagen (type I)-coated dishes (Asahi Techno Glass, Tokyo, Japan), and then hepatic induction was performed over a period of three weeks by culturing in a HCM-modified William's E medium containing: transferrin (5 μ g/ml), hydrocortisone-21-hemisuccinate (10^{-6} M), bovine serum albumin (0.5mg/ml), ascorbic acid (2mM), epidermal growth factor (20ng/ml), insulin (5 μ g/ml) gentamicin (50 μ g/ml) (Cambrex) and dexamethasone (10^{-8} M) and supplemented with HIFC that contained HGF (150ng/ml), FGF1 (300ng/ml), and FGF4 (25ng/ml) (PeproTech EC, London, UK) (Fig. 1B). For the next two weeks, the cells were treated with OsM (30ng/ml) and dexamethasone (2×10^{-5} mol/l) and then cultured in HCM alone for 2-5 weeks. Hepatic differentiation was identified by cell morphology, immunohistochemistry, RT-PCR analysis, Western blot analysis, and biochemical functions. All were performed